

The effects of non-helical component of hypermagnetic field on the evolution of the matter-antimatter asymmetry, vorticity, and hypermagnetic field

Saeed Abbaslu
Dr. S. Rostam Zadeh
Dr. S. S. Gousheh
A. Rezaei

August 17, 2022

- Introduction
- Chiral Vortical Effect (CVE) and Chiral Magnetic Effect (CME)
- Anomalous Magneto Hydro Dynamics (AMHD)
- Non Helical Hyper Magnetic Field (NHHMF)
- Results

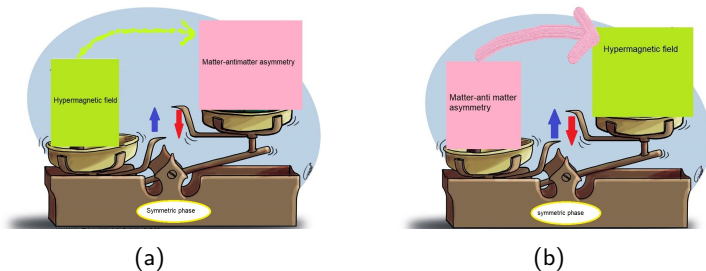
Magnetic field:

- The Universe is magnetized on all scales that we have observed so far, planets, stars, galaxies, and galaxy clusters.
- galaxies $\rightarrow B \sim 10^{-6}G$ &, $\lambda_c \sim kpc$.
- Intra-cluster medium (ICM) in clusters $\rightarrow B \sim (1 - 10)10^{-6}G$ &, $\lambda_c \sim (10 - 100)kpc$.
- Intergalactic medium (IGM) $\rightarrow B \sim (10^{-16} - 10^{-9})G$ &, $\lambda_c \sim Mpc$.

Magnetogenesis models:

- Astrophysical models (Biermann Battery mechanism, Dynamo Mechanism ,...)
- Models based on early universe processes (Inflationary scenario, Phase transition, [Asymmetries in the early Universe](#))

In fact, the matter-antimatter asymmetry generation and the (hyper)magnetogenesis are strongly intertwined via these hypercharge Abelian anomalous effects, $\partial_{\mu}j^{\mu} \sim Y_{\mu\nu}\tilde{Y}^{\mu\nu} \sim \vec{E}_Y \cdot \vec{B}_Y$.



Baryon asymmetry:

- Our Universe contains more matter (baryons) than the antimatter (antibaryons) with the measured baryon asymmetry of the order $\eta \sim 10^{-10}$.
- Sakharov stated three necessary conditions for generating the BAU:
 - (i) baryon number violation,
 - (ii) C and CP violation,
 - (iii) departure from thermal equilibrium.



Anomalous current:

- **CME:** The chiral magnetic effect refers to the generation of an electric current parallel to the magnetic field in an imbalanced chiral plasma, $J_{\text{cm,r}}^\mu = \frac{rQ_r^2}{4\pi^2} \mu_r \vec{B}_Y$.
- **CVE:** The chiral vortical effect, generically induced by the rotation of chiral matter, refers to the generation of an electric current parallel to the vorticity field, $\vec{J}_{\text{cv,r}} = rQ_r \left(\frac{T^2}{24} + \frac{\mu_r^2}{8\pi^2} \right) \vec{\omega}$.

In presence of these anomalous currents the ordinary Magneto Hydro Dynamic equations (MHD) promote to the Anomalous Magneto Hydro Dynamic (AMHD) equations.

Anomalous MagnetohydroDynamics:

The energy-momentum tensor $T^{\mu\nu}$ and the total electric current J^μ are given by

$$T^{\mu\nu} = (\rho + p)u^\mu u^\nu - pg^{\mu\nu} + \frac{1}{4}g^{\mu\nu}F^{\alpha\beta}F_{\alpha\beta} - F^{\nu\sigma}F^\mu{}_\sigma + \tau^{\mu\nu}, \quad (1)$$

$$J^\mu = \rho_{\text{el}}u^\mu + J_{\text{cm}}^\mu + J_{\text{cv}}^\mu + \nu^\mu, \quad (2)$$

$$J_{\text{cm}}^\mu = \sum_{i=l,q} (Q_{R_i}\xi_{B,R_i} + Q_{L_i}\xi_{B,L_i})B^\mu = c_B B^\mu, \quad (3)$$

$$J_{\text{cv}}^\mu = \sum_{i=l,q} (Q_{R_i}\xi_{v,R_i} + Q_{L_i}\xi_{v,L_i})\omega^\mu = c_v \omega^\mu \quad (4)$$

$$\nu^\mu = \sigma E^\mu \quad (5)$$

where, $u^\mu = \gamma(1, \vec{v}/R)$ is the four-velocity of the plasma normalized such that $u^\mu u_\mu = 1$. ν^μ and $\tau^{\mu\nu}$ denote the electric diffusion current and viscous stress tensor, respectively. $B^\mu = (\epsilon^{\mu\nu\rho\sigma}/2R^3)u_\nu F_{\rho\sigma}$ is the magnetic field four-vector, $E^\mu = F^{\mu\nu}u_\nu$ is the electric field four-vector, and $\omega^\mu = (\epsilon^{\mu\nu\rho\sigma}/R^3)u_\nu \nabla_\rho u_\sigma$ is the vorticity four-vector, with the totally anti-symmetric Levi-Civita tensor density specified by $\epsilon^{0123} = -\epsilon_{0123} = 1$.

$$\xi_{B,R} = \frac{Q_R \mu_R}{4\pi^2} \left[1 - \frac{1}{2} \frac{n_R \mu_R}{\rho + p} \right] - \frac{1}{24} \frac{n_R T^2}{\rho + p} \simeq \frac{Q_R \mu_R}{4\pi^2}, \quad (6)$$

$$\xi_{B,L} = -\frac{Q_L \mu_L}{4\pi^2} \left[1 - \frac{1}{2} \frac{n_L \mu_L}{\rho + p} \right] + \frac{1}{24} \frac{n_L T^2}{\rho + p} \simeq -\frac{Q_L \mu_L}{4\pi^2}, \quad (7)$$

$$\xi_{v,R} = \frac{\mu_R^2}{8\pi^2} \left[1 - \frac{2}{3} \frac{n_R \mu_R}{\rho + p} \right] + \frac{1}{24} T^2 \left[1 - \frac{2n_R \mu_R}{\rho + p} \right] \simeq \frac{\mu_R^2}{8\pi^2} + \frac{1}{24} T^2, \quad (8)$$

$$\xi_{v,L} = -\frac{\mu_L^2}{8\pi^2} \left[1 - \frac{2}{3} \frac{n_L \mu_L}{\rho + p} \right] - \frac{1}{24} T^2 \left[1 - \frac{2n_L \mu_L}{\rho + p} \right] \simeq -\frac{\mu_L^2}{8\pi^2} - \frac{1}{24} T^2. \quad (9)$$

The equations of AMHD consist of:

- The Maxwell's equations:

$$\begin{aligned}\nabla_{\mu} F^{\mu\nu} &= J^{\nu}, & F_{\mu\nu} &= \nabla_{\mu} A_{\nu} - \nabla_{\nu} A_{\mu} \\ \nabla_{\mu} \tilde{F}^{\mu\nu} &= 0, & \tilde{F}^{\mu\nu} &= \frac{1}{2R^3} \epsilon^{\mu\nu\alpha\beta} F_{\alpha\beta},\end{aligned}\tag{10}$$

- The energy-momentum conservation

$$\nabla_{\mu} T^{\mu\nu} = 0,\tag{11}$$

- Anomaly equations:

$$\nabla_{\mu} j_{R,L}^{\mu} = C_{R,L} E_{\mu} B^{\mu},\tag{12}$$

$$\begin{aligned}j_{R}^{\mu} &= n_{R} u^{\mu} + \xi_{B,R} B^{\mu} + \xi_{v,R} \omega^{\mu} + V_{R}^{\mu}, \\ j_{L}^{\mu} &= n_{L} u^{\mu} + \xi_{B,L} B^{\mu} + \xi_{v,L} \omega^{\mu} + V_{L}^{\mu},\end{aligned}\tag{13}$$

where ∇_{μ} is the covariant derivative with respect to the Friedmann-Robertson-Walker (FRW) metric $ds^2 = dt^2 - R^2(t)\delta_{ij}dx^i dx^j$.

Maxwell's equations: $\nabla_{\mu} F^{\mu\nu} = J^{\nu}$, $\nabla_{\mu} \tilde{F}^{\mu\nu} = 0$

$$\frac{1}{R} \vec{\nabla} \cdot \vec{E}_Y = 0, \quad \frac{1}{R} \vec{\nabla} \cdot \vec{B}_Y = 0, \quad (14)$$

$$\frac{1}{R} \vec{\nabla} \times \vec{E}_Y + \left(\frac{\partial \vec{B}_Y}{\partial t} + 2H \vec{B}_Y \right) = 0, \quad (15)$$

$$\frac{1}{R} \vec{\nabla} \times \vec{B}_Y - \left(\frac{\partial \vec{E}_Y}{\partial t} + 2H \vec{E}_Y \right) = \vec{J} \quad (16)$$

$$\vec{J} = \vec{J}_{\text{Ohm}} + \vec{J}_{\text{cm}} + \vec{J}_{\text{cv}},$$

$$\vec{J}_{\text{Ohm}} = \sigma \left(\vec{E}_Y + \vec{v} \times \vec{B}_Y \right), \quad (17)$$

$$\vec{J}_{\text{cm}} = c_B \vec{B}_Y, \quad (18)$$

$$\vec{J}_{\text{cv}} = c_v \vec{\omega}, \quad (19)$$

$$\vec{\omega} = \frac{1}{R} \vec{\nabla} \times \vec{v}, \quad (20)$$

CVE and CME coefficients:

$$c_v(t) = \sum_{i=1}^{n_G} \left[\frac{g'}{48} \left(-Y_R T_{R_i}^2 + Y_L T_{L_i}^2 N_w - Y_{dR} T_{dR_i}^2 N_c - Y_{uR} T_{uR_i}^2 N_c + Y_Q T_{Q_i}^2 N_c N_w \right) \right. \\ \left. + \frac{g'}{16\pi^2} \left(-Y_R \mu_{R_i}^2 + Y_L \mu_{L_i}^2 N_w - Y_{dR} \mu_{dR_i}^2 N_c - Y_{uR} \mu_{uR_i}^2 N_c + Y_Q \mu_{Q_i}^2 N_c N_w \right) \right], \quad (21)$$

$$c_B(t) = -\frac{g'^2}{8\pi^2} \sum_{i=1}^{n_G} \left[-\left(\frac{1}{2}\right) Y_R^2 \mu_{R_i} - \left(\frac{-1}{2}\right) Y_L^2 \mu_{L_i} N_w - \left(\frac{1}{2}\right) Y_{dR}^2 \mu_{dR_i} N_c \right. \\ \left. - \left(\frac{1}{2}\right) Y_{uR}^2 \mu_{uR_i} N_c - \left(\frac{-1}{2}\right) Y_Q^2 \mu_{Q_i} N_c N_w \right], \quad (22)$$

$$Y_L = -1, \quad Y_R = -2, \quad Y_Q = \frac{1}{3}, \quad Y_{uR} = \frac{4}{3}, \quad Y_{dR} = -\frac{2}{3}. \quad (23)$$

Here for simplicity we assume that $\mu_{uR} = \mu_{dR} = \mu_Q$ and obtain $\mu_B = 12\mu_Q$. Therefore the above equation simplifies to

$$c_v(t) = \frac{g'}{8\pi^2} \left(\mu_{eR}^2 - \mu_{eL}^2 \right), \quad c_B(t) = -\frac{g'^2}{8\pi^2} \left(-2\mu_{eR} + \mu_{eL} - \frac{3}{4}\mu_B \right), \quad (24)$$

Continuity and Navier-Stokes equations: $\nabla_\mu T^\mu = 0$

$$\frac{\partial \rho}{\partial t} + \frac{1}{R} \vec{\nabla} \cdot [(\rho + p) \vec{v}] + 3H(\rho + p) = 0, \quad (25)$$

$$\left[\frac{\partial}{\partial t} + \frac{1}{R} (\vec{v} \cdot \vec{\nabla}) + H \right] \vec{v} + \frac{\vec{v}}{\rho + p} \frac{\partial p}{\partial t} = \quad (26)$$

$$- \frac{1}{R} \frac{\vec{\nabla} p}{\rho + p} + \frac{\vec{J} \times \vec{B}_Y}{\rho + p} + \frac{\nu}{R^2} \left[\nabla^2 \vec{v} + \frac{1}{3} \vec{\nabla} (\vec{\nabla} \cdot \vec{v}) \right],$$

Due to the homogeneity of the Universe, we can ignore the gradient of the pressure in the evolution equation of the momentum, and obtain the evolution of the velocity for incompressible fluid, $\vec{\nabla} \cdot \vec{v} = 0$ as follow:

$$\frac{\partial \vec{v}}{\partial t} = \frac{\vec{J} \times \vec{B}_Y}{\rho + p} + \frac{\nu}{R^2} \nabla^2 \vec{v}, \quad (27)$$

$$\nu \simeq 1/(5\alpha_Y T)$$

Anomaly equations: $\nabla_\mu j_{R,L}^\mu = C_{R,L} E_\mu B^\mu = -C_{R,L} \vec{E}_Y \cdot \vec{B}_Y,$

$$\begin{aligned} j_{(R,L)}^0 &= (n_{R,L} - \bar{n}_{R,L}) + \xi_{B,(R,L)} \vec{v} \cdot \vec{B}_Y + \xi_{v,(R,L)} \vec{v} \cdot \vec{\omega} + \sigma_{(R,L)} \vec{v} \cdot \vec{E}_Y, \\ \vec{j}_{(R,L)} &= (n_{R,L} - \bar{n}_{R,L}) \vec{v} + \xi_{B,(R,L)} \vec{B}_Y + \xi_{v,(R,L)} \vec{\omega} + \sigma_{(R,L)} (\vec{E}_Y + \vec{v} \times \vec{B}_Y). \end{aligned} \quad (28)$$

After taking the spatial average of anomaly equation, the divergent terms $\frac{1}{R} \vec{\nabla} \cdot \vec{j}_{(R,L)}$ will be vanish. By using the relation $\langle \vec{E}_Y \cdot \vec{B}_Y \rangle = -\frac{1}{2} (\partial_t + 3H) \langle \vec{A}_Y \cdot \vec{B}_Y \rangle$, we can write

$$\partial_t \left[\eta_{R,L} + \frac{\xi_{B,(R,L)}}{s} \langle \vec{v} \cdot \vec{B}_Y \rangle + \frac{\xi_{v,(R,L)}}{s} \langle \vec{v} \cdot \vec{\omega} \rangle + \frac{\sigma_{(R,L)}}{s} \langle \vec{v} \cdot \vec{E}_Y \rangle - \frac{C_{R,L}}{2s} \langle \vec{A}_Y \cdot \vec{B}_Y \rangle \right] = 0, \quad (29)$$

where $\eta_i = (n_i - \bar{n}_i)/s$, $s = (2\pi^2 g^* T^3)/45$ is entropy, and $g^* = 106.75$ is the number of relativistic degrees of freedom. High temperature of the early Universe plasma and low-velocity limit imply that

$$\partial_t \eta_{R,L} \simeq \partial_t \left[\frac{C_{R,L}}{2s} \langle \vec{A}_Y \cdot \vec{B}_Y \rangle \right], \quad (30)$$

$$\frac{d\eta_{eR}}{dt} = \frac{g'^2}{4\pi^2 s} \langle \vec{E}_Y \cdot \vec{B}_Y \rangle + 2\Gamma_{RL} (\eta_{eL} - \eta_{eR}), \quad (31)$$

$$\frac{d\eta_{eL}}{dt} = \frac{d\eta_{\nu_e^L}}{dt} = -\frac{g'^2}{16\pi^2 s} \langle \vec{E}_Y \cdot \vec{B}_Y \rangle + \Gamma_{RL} (\eta_{eR} - \eta_{eL}),$$

$$\Gamma_{RL} = \left(\frac{\Gamma_0}{2t_{EW}} \right) \left(\frac{1-x}{\sqrt{x}} \right), \quad (32)$$

where the variable $x = \frac{t}{t_{EW}} = \left(\frac{T_{EW}}{T} \right)^2$, $t_{EW} = \frac{M_0}{2T_{EW}^2}$, $M_0 = M_{Pl}/1.66\sqrt{g^*}$, and M_{Pl} is the Plank mass, and $\Gamma_0 = 121$.

$$\eta_B/3 - \eta_{L_i} = \text{const.} \rightarrow \frac{1}{3} \frac{d\eta_B}{dt} = \frac{d\eta_{eR}}{dt} + 2 \frac{d\eta_{eL}}{dt} = \frac{g'^2}{8\pi^2 s} \langle \vec{E}_Y \cdot \vec{B}_Y \rangle. \quad (33)$$

$$\langle \vec{E}_Y \cdot \vec{B}_Y \rangle = ? \quad (34)$$

$$\vec{E}_Y = \frac{1}{\sigma R} \vec{\nabla} \times \vec{B}_Y - \frac{c_v}{\sigma} \vec{\omega} - \frac{c_B}{\sigma} \vec{B}_Y - \vec{v} \times \vec{B}_Y. \quad (35)$$

$$\langle \vec{E}_Y \cdot \vec{B}_Y \rangle = \frac{1}{\sigma R} \langle \vec{B}_Y \cdot \vec{\nabla} \times \vec{B}_Y \rangle - \frac{c_v}{\sigma} \langle \vec{B}_Y \cdot \vec{\omega} \rangle - \frac{c_B}{\sigma} \langle \vec{B}_Y \cdot \vec{B}_Y \rangle. \quad (36)$$

$$\frac{\partial \vec{B}_Y}{\partial t} = \frac{1}{\sigma R^2} \nabla^2 \vec{B}_Y + \frac{c_v}{\sigma R} \vec{\nabla} \times \vec{\omega} + \frac{c_B}{\sigma R} \vec{\nabla} \times \vec{B}_Y + \frac{1}{R} \vec{\nabla} \times (\vec{v} \times \vec{B}_Y) - \frac{\vec{B}_Y}{t}, \quad (37)$$

$$\vec{\omega} = \vec{\nabla} \times \vec{v},$$

$$\frac{\partial \vec{v}}{\partial t} = \frac{\vec{J} \times \vec{B}_Y}{\rho + p} + \frac{\nu}{R^2} \nabla^2 \vec{v}, \quad (38)$$

The non-helical hypermagnetic field, vorticity and asymmetry

Since $\vec{\nabla} \cdot \vec{B}_Y = 0$, the hypermagnetic field can be written as $\vec{B}_Y = (1/R)\vec{\nabla} \times \vec{A}_Y$, where \vec{A}_Y is the vector potential of the hypermagnetic field. For incompressible fluid, $\vec{\nabla} \cdot \vec{v} = 0$, in analogy with the hypermagnetic field, the velocity field can be written as $\vec{v} = (1/R)\vec{\nabla} \times \vec{S}$, where \vec{S} is the vector potential of the velocity field. Now we choose the configurations for our hypermagnetic field and the velocity field by using the following orthonormal basis $\{\hat{a}(z, k) = (\cos kz, -\sin kz, 0), \hat{b}(z, k) = (\sin kz, \cos kz, 0), \hat{z}\}$.

$$\vec{B}_Y(t, z) = B_z(t)\hat{z} + B_a(t)\hat{a}(z, k) + B_b(t)\hat{b}(z, k), \quad (39)$$

$$\vec{v}(t, z) = v_a(t)\hat{a}(z, k) + v_b(t)\hat{b}(z, k), \quad (40)$$

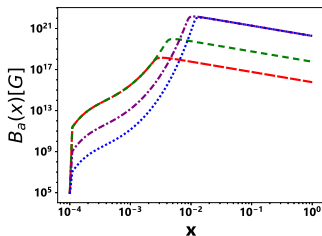
$$\frac{1}{R}\vec{\nabla} \times (\vec{v} \times \vec{B}_Y) \neq 0, \quad \text{and} \quad \frac{\vec{J} \times \vec{B}_Y}{\rho + p} \neq 0 \quad (41)$$

$$\begin{aligned} \langle \vec{E}_Y \cdot \vec{B}_Y \rangle &= -\frac{c_B}{\sigma} [B_z^2(t) + B_a^2(t) + B_b^2(t)] + \frac{k'}{\sigma} [B_a^2(t) + B_b^2(t)] \\ &\quad - \frac{c_v}{\sigma} k' [v_a(t)B_a(t) + v_b(t)B_b(t)]. \end{aligned} \quad (42)$$

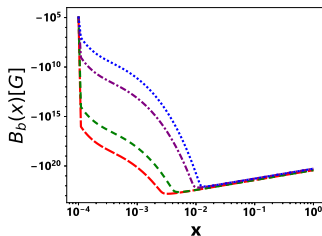
$$\begin{aligned}
 \frac{\partial B_a(t)}{\partial t} &= k' [v_b(t)B_z(t)] + \left[-\frac{k'^2}{\sigma} + \frac{k'c_B}{\sigma} \right] B_a(t) + \frac{k'^2 c_v}{\sigma} v_a(t) - \frac{B_a(t)}{t}, \\
 \frac{\partial B_b(t)}{\partial t} &= -k' [v_a(t)B_z(t)] + \left[-\frac{k'^2}{\sigma} + \frac{k'c_B}{\sigma} \right] B_b(t) + \frac{k'^2 c_v}{\sigma} v_b(t) - \frac{B_b(t)}{t}, \\
 \frac{\partial B_z(t)}{\partial t} &= -\frac{B_z(t)}{t}, \\
 \frac{\partial v_a(t)}{\partial t} &= \frac{k'}{\rho + p} [B_b(t)B_z(t)] - k'^2 \nu v_a(t), \\
 \frac{\partial v_b(t)}{\partial t} &= -\frac{k'}{\rho + p} [B_a(t)B_z(t)] - k'^2 \nu v_b(t).
 \end{aligned} \tag{43}$$

$$\begin{aligned}\frac{d\eta_{e_R}}{dt} &= \frac{g'^2}{4\pi^2 s} \langle \vec{E}_Y \cdot \vec{B}_Y \rangle + \left(\frac{\Gamma_0}{t_{EW}} \right) \left(\frac{1-x}{\sqrt{x}} \right) (\eta_{e_L} - \eta_{e_R}), \\ \frac{d\eta_{e_L}}{dt} &= \frac{d\eta_{\nu_e}^L}{dt} = -\frac{g'^2}{16\pi^2 s} \langle \vec{E}_Y \cdot \vec{B}_Y \rangle + \left(\frac{\Gamma_0}{2t_{EW}} \right) \left(\frac{1-x}{\sqrt{x}} \right) (\eta_{e_R} - \eta_{e_L}), \\ \frac{1}{3} \frac{d\eta_B}{dt} &= \frac{d\eta_{e_R}}{dt} + 2 \frac{d\eta_{e_L}}{dt},\end{aligned}\tag{44}$$

First scenario:



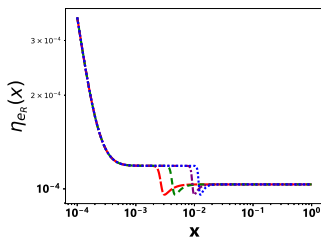
(c)



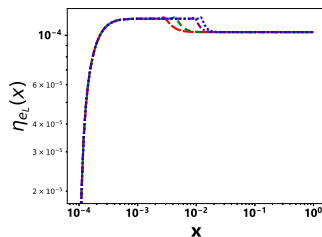
(d)

Figure: The time plots of the helical components $B_a(x)$ and $B_b(x)$, with the initial conditions $B_a^{(0)} = B_b^{(0)} = 0$, $\eta_{eR}^{(0)} = 3.56 \times 10^{-4}$, and $\eta_{eL}^{(0)} = \eta_B^{(0)} = 0$. Large (red) dashed line is for $v_a^{(0)} = 10^{-7}$, $v_b^{(0)} = 10^{-14}$, and $B_z^{(0)} = 10^{19}$ G, dashed (green) line for $v_a^{(0)} = 10^{-7}$, $v_b^{(0)} = 10^{-14}$, and $B_z^{(0)} = 10^{17}$ G, dotted-dashed (violet) line for $v_a^{(0)} = v_b^{(0)} = 10^{-14}$, and $B_z^{(0)} = 10^{19}$ G, and dotted (blue) line for $v_a^{(0)} = v_b^{(0)} = 10^{-14}$, and $B_z^{(0)} = 10^{17}$ G.

First scenario:



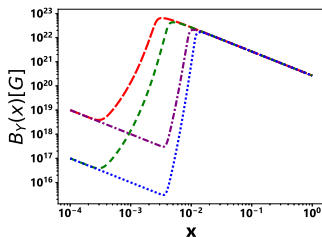
(a)



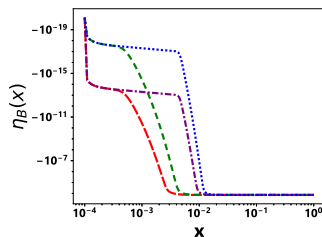
(b)

Figure: The time plots of the the right-handed electron asymmetry $\eta_{eR}(x)$, the left-handed electron asymmetry $\eta_{eL}(x)$ with the initial conditions $B_a^{(0)} = B_b^{(0)} = 0$, $\eta_{eR}^{(0)} = 3.56 \times 10^{-4}$, and $\eta_{eL}^{(0)} = \eta_B^{(0)} = 0$. Large (red) dashed line is for $v_a^{(0)} = 10^{-7}$, $v_b^{(0)} = 10^{-14}$, and $B_z^{(0)} = 10^{19} \text{G}$, dashed (green) line for $v_a^{(0)} = 10^{-7}$, $v_b^{(0)} = 10^{-14}$, and $B_z^{(0)} = 10^{17} \text{G}$, dotted-dashed (violet) line for $v_a^{(0)} = v_b^{(0)} = 10^{-14}$, and $B_z^{(0)} = 10^{19} \text{G}$, and dotted (blue) line for $v_a^{(0)} = v_b^{(0)} = 10^{-14}$, and $B_z^{(0)} = 10^{17} \text{G}$.

First scenario:



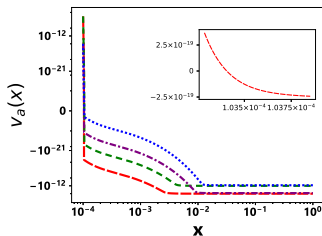
(a)



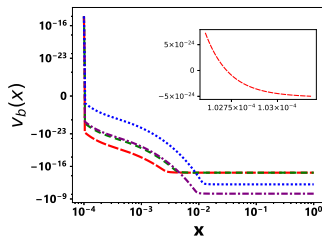
(b)

Figure: The time plots of the hypermagnetic field amplitude $B_Y(x)$, and the baryon asymmetry $\eta_B(x)$ with the initial conditions $B_a^{(0)} = B_b^{(0)} = 0$, $\eta_{eR}^{(0)} = 3.56 \times 10^{-4}$, and $\eta_{eL}^{(0)} = \eta_B^{(0)} = 0$. Large (red) dashed line is for $v_a^{(0)} = 10^{-7}$, $v_b^{(0)} = 10^{-14}$, and $B_z^{(0)} = 10^{19}$ G, dashed (green) line for $v_a^{(0)} = 10^{-7}$, $v_b^{(0)} = 10^{-14}$, and $B_z^{(0)} = 10^{17}$ G, dotted-dashed (violet) line for $v_a^{(0)} = v_b^{(0)} = 10^{-14}$, and $B_z^{(0)} = 10^{19}$ G, and dotted (blue) line for $v_a^{(0)} = v_b^{(0)} = 10^{-14}$, and $B_z^{(0)} = 10^{17}$ G.

First scenario:



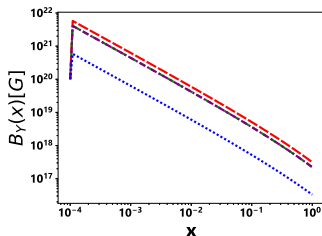
(a)



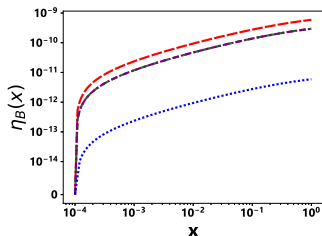
(b)

Figure: The time plots of the $v_a(x)$ and $v_b(x)$ with the initial conditions $B_a^{(0)} = B_b^{(0)} = 0$, $\eta_{eR}^{(0)} = 3.56 \times 10^{-4}$, and $\eta_{eL}^{(0)} = \eta_B^{(0)} = 0$. Large (red) dashed line is for $v_a^{(0)} = 10^{-7}$, $v_b^{(0)} = 10^{-14}$, and $B_z^{(0)} = 10^{19}$ G, dashed (green) line for $v_a^{(0)} = 10^{-7}$, $v_b^{(0)} = 10^{-14}$, and $B_z^{(0)} = 10^{17}$ G, dotted-dashed (violet) line for $v_a^{(0)} = v_b^{(0)} = 10^{-14}$, and $B_z^{(0)} = 10^{19}$ G, and dotted (blue) line for $v_a^{(0)} = v_b^{(0)} = 10^{-14}$, and $B_z^{(0)} = 10^{17}$ G.

Second scenario:



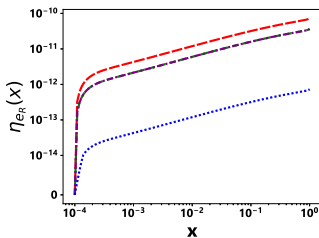
(a)



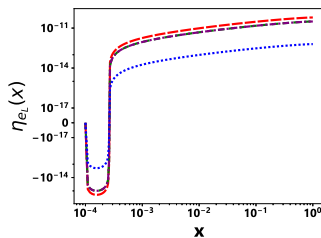
(b)

Figure: The time plots of the hypermagnetic field amplitude $B_Y(x)$, the baryon asymmetry $\eta_B(x)$, in the presence of the viscosity, with the initial conditions $B_z^{(0)} = 10^{20} \text{G}$, $B_a^{(0)} = B_b^{(0)} = 0$, and $\eta_{eR}^{(0)} = \eta_{eL}^{(0)} = \eta_B^{(0)} = 0$. Large dashed (red) line is for, $v_a^{(0)} = v_b^{(0)} = 10^{-2}$, dashed (green) line for $v_a^{(0)} = 10^{-2}$, $v_b^{(0)} = 0$, dot-dashed (violet) line for $v_a^{(0)} = 0$, $v_b^{(0)} = 10^{-2}$, and dotted (blue) line for $v_a^{(0)} = v_b^{(0)} = 10^{-3}$.

Second scenario:



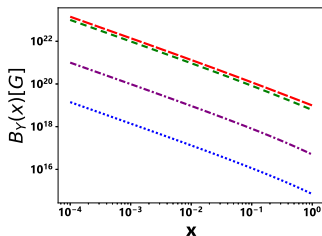
(a)



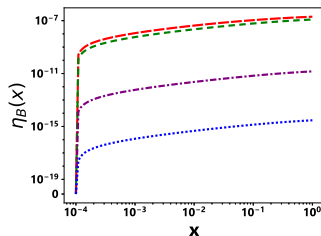
(b)

Figure: The time plots of the the right-handed electron asymmetry $\eta_{eR}(x)$, the left-handed electron asymmetry $\eta_{eL}(x) \simeq \eta_{\nu_L}(x)$, in the presence of the viscosity, with the initial conditions $B_z^{(0)} = 10^{20} \text{G}$, $B_a^{(0)} = B_b^{(0)} = 0$, and $\eta_{eR} = \eta_{eL} = \eta_B^{(0)} = 0$. Large dashed (red) line is for, $v_a^{(0)} = v_b^{(0)} = 10^{-2}$, dashed (green) line for $v_a^{(0)} = 10^{-2}$, $v_b^{(0)} = 0$, dot-dashed (violet) line for $v_a^{(0)} = 0$, $v_b^{(0)} = 10^{-2}$, and dotted (blue) line for $v_a^{(0)} = v_b^{(0)} = 10^{-3}$.

Third scenario:



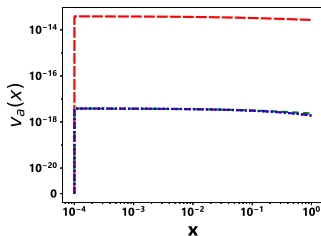
(a)



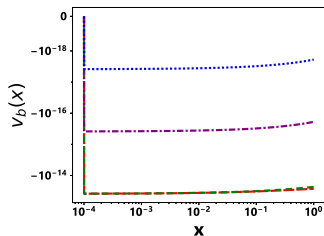
(b)

Figure: The time plots of the the hypermagnetic field amplitude $B_Y(x)$, the baryon asymmetry $\eta_B(x)$, with the initial conditions $B_z^{(0)} = 10^{17} \text{G}$, and $\eta_{e_R}^{(0)} = \eta_{e_L}^{(0)} = \eta_B^{(0)} = v_a^{(0)} = v_b^{(0)} = 0$. Large (red) dashed line is for $B_a^{(0)} = B_b^{(0)} = 10^{23} \text{G}$, dashed (green) line for $B_a^{(0)} = 10^{23} \text{G}$, $B_b^{(0)} = 10^{19} \text{G}$, dotted-dashed (violet) line for $B_a^{(0)} = 10^{21} \text{G}$, $B_b^{(0)} = 10^{19} \text{G}$, and dotted (blue) line for $B_a^{(0)} = B_b^{(0)} = 10^{19} \text{G}$.

Third scenario:



(a)



(b)

Figure: The time plots of the velocity fields amplitude $v_a(x)$ and $v_b(x)$, with the initial conditions $B_z^{(0)} = 10^{17} \text{G}$, and $\eta_{eR}^{(0)} = \eta_{eL}^{(0)} = \eta_B^{(0)} = v_a^{(0)} = v_b^{(0)} = 0$. Large (red) dashed line is for $B_a^{(0)} = B_b^{(0)} = 10^{23} \text{G}$, dashed (green) line for $B_a^{(0)} = 10^{23} \text{G}$, $B_b^{(0)} = 10^{19} \text{G}$, dotted-dashed (violet) line for $B_a^{(0)} = 10^{21} \text{G}$, $B_b^{(0)} = 10^{19} \text{G}$, and dotted (blue) line for $B_a^{(0)} = B_b^{(0)} = 10^{19} \text{G}$.

$$B_A = B_Y \cos \theta_W \simeq 0.88 B_Y$$

$$B_Y(T_{EW}) \sim 10^{17-20} G \quad (45)$$

$$\eta_B = (n_B - \bar{n}_B)/s$$

$$s = 2\pi^2 g^* T^3/45, \quad g^*(T > T_{EW}) = 106.75$$

$$g_0^* = 43/11$$

$$\eta_B(T_0) = 27.3 \times \eta_B(T_{EW}) \quad (46)$$

$$10^{-15} < \eta_B(T_{EW}) < 10^{-8}$$

$$\eta_{BBN} = 5.8 \pm 0.27 \times 10^{-10}$$

$$\eta_{CMB} = 6.16 \pm 0.15 \times 10^{-10}$$

- In this study, the hypermagnetic field configurations which include both helical and non-helical components, are considered. It is shown that in the presence of weak vorticity and a large right-handed electron asymmetry, the helicity can be generated and amplified for an initially non-helical hypermagnetic field. The vorticity also grows, even in the presence of the viscosity, in contrast to the case in which a fully-helical hypermagnetic field is assumed. In a different scenario it is also shown that in the presence of a strong non-helical hypermagnetic field and large vorticity, helicity and baryon asymmetry can be generated and amplified.

- [1] S. Abbaslu, S. Rostam Zadeh and S. S. Gousheh, "Contribution of the chiral vortical effect to the evolution of the hypermagnetic field and the matter-antimatter asymmetry in the early Universe," Phys. Rev. D **100**, no.11, 116022 (2019), [arXiv:1908.10105 [hep-ph]].
- [2] S. Abbaslu, S. Rostam Zadeh, A. Rezaei and S. S. Gousheh, "The effects of non-helical component of hypermagnetic field on the evolution of the matter-antimatter asymmetry, vorticity, and hypermagnetic field," Phys. Rev. D **104**, no.5, 056028 (2021) [arXiv:2104.05013 [hep-ph]].
- [3] S. Abbaslu, S. R. Zadeh, M. Mehraeen and S. S. Gousheh, "The generation of matter-antimatter asymmetries and hypermagnetic fields by the chiral vortical effect of transient fluctuations," Eur. Phys. J. C **81**, no.6, 500 (2021) [arXiv:2001.03499 [hep-ph]].
- [4] S. Abbaslu, S. R. Zadeh and S. S. Gousheh, "Contribution of the thermal mass to the chiral vortical effect and magnetobaryogenesis," [arXiv:2108.10035 [hep-ph]].

Thank you for your attention